Automatic Estimation of Boresight Angles Between IMU and Multi-Beam Echo Sounder Sytems

Nicolas Seube, Sébastien Levilly and Kees de Jong

Abstract Nowadays, the boresight calibration between IMU (Inertial Measurement Unit) and MBES (Multi-Beam Echo Sounder) systems is achieved by the patch-test procedure which estimates the three boresight angles: roll, pitch and yaw. That procedure consists in two steps. The first one is the selection of an overlapping area. That selection is done thanks to the experience of a surveyor. The second step evaluates the roll, pitch and yaw angles separately by a method which tries a subset of possible angles. For theses possible angles, the discrepancy between digital terrain models (one DTM by survey line) is calculated in the previous selected area and the minimum is assumed to be the "optimal" solution. This paper presents some preleminary results from a research project between FUGRO, ENSTA Bretagne and CIDCO. This project aim is to design new methods in the calibration topic. These procedures use multi-dimensional optimization concepts in order to provide statistical analysis which should appear in any calibration report.

1 Introduction

We consider the problem of boresight calibration of a hydrographic system, composed by a Multi-Beam Echo Sounder (MBES), an Inertial Measurement Unit (IMU) and a positioning system (generally being a GNSS receiver). This hydrographic system, as all mobile mapping systems, enables one to determine the position of soundings in a geographic frame from the knowledge of raw source data from the MBES,

Kees de Jong—Deceased

N. Seube (✉)
CIDCO, Rimouski, Canada
e-mail: nicolas.seube@cidco.ca

S. Levilly
ENSTA Bretagne, Brest, France
e-mail: sebastien.levilly@ensta-bretagne.org

K. de Jong
Fugro Intersite B.V., Leidschendam, The Netherlands

B. Zerr et al. (eds.), *Quantitative Monitoring of the Underwater Environment*,
Ocean Engineering & Oceanography 6, DOI 10.1007/978-3-319-32107-3_2

IMU and GNSS receiver. This can be done by using a spatial referencing equation and a simplified version is the following Eq. (1).

$$\mathbf{X}_n(t) = \mathbf{P}_n(t) + C_{bI}^{n}(t - dt)[C_{bS}^{bI}\mathbf{r}_{bS}(t) + \mathbf{a}_{bI}] \tag{1}$$

where $\mathbf{X}_n = (x, y, z)_n$ is the position of a sounding in a navigation frame *(n)* (which can be a local geodetic frame), $\mathbf{P}_n$ is the position delivered by the GNSS receiver in frame *(n)*, C_{bI}^{n} is the coordinate transformation from the IMU body frame to the navigation frame (which can be parametrized using Euler angles (φ, θ, ψ), denoting roll, pitch and yaw, respectively), the MBES return r_{bS}, coordinated in the MBES frame *(bS)*, the lever-arm vector coordinated in the IMU frame a_{bI} and the boresight coordinate transformation C_{bS}^{bI}.

In Eq. (1), t denotes the reference time from the GNSS, which is supposed to be propagated to the IMU through a distributed time and message synchronization system [1], and dt denotes a possible latency between the MBES and the IMU.

The dependency of the calibration parameters on soundings spatial referencing is described by Eq. (1), among them are:

- dt, the latency between the IMU and the MBES system (it is to be noticed that in most modern hydrographic systems, latency between GNSS and the MBES impact can be considered as negligible, but latency between the MBES and IMU is not [9];
- C_{bS}^{bI}, the boresight coordinate transformation;
- $\mathbf{a}_{bI}$, the lever-arms which may be affected by static measurement errors, coordinate transformation errors from the measurement frame to the IMU frame, and in some cases, time-varying (for large ships for instance);
- The MBES range and beam launch angles, affecting the term $\mathbf{r}_{bS}$.

This article will focus on the estimation of boresight coordinate transformation C_{bS}^{bI}, as an essential component of calibration parameters. A classical method to determine this transformation is the so-called "patch-test" which principle is briefly recalled here and which limitations are hereafter detailed. The patch-test decouples the three boresight angles estimation problem, and starts with the roll angle, followed by the pitch, and then the yaw angle. For the roll angle, a flat bottom, surveyed in opposite direction is used, since the roll boresight $\delta\varphi$ effect can be easily characterized (see Fig. 1).

We illustrate the pitch boresight calibration method, which uses nadir data from two opposite lines over a slope. Figure 2 illustrates the effect of a pitch boresight $\delta\theta$ over a regular slope, followed by a flat terrain.

The estimation of the yaw boresight is classically done by identifying a target over a flat bottom, and by surveying this target using two lines in the same direction, with outer beams intersecting the target. In order to improve the resolution of this method (which may suffer from the fact that the target size may not be significant enough, which causes uncertainty on the tie point position precision and accuracy), one can also survey two parallel lines in the same direction over a regular slope.

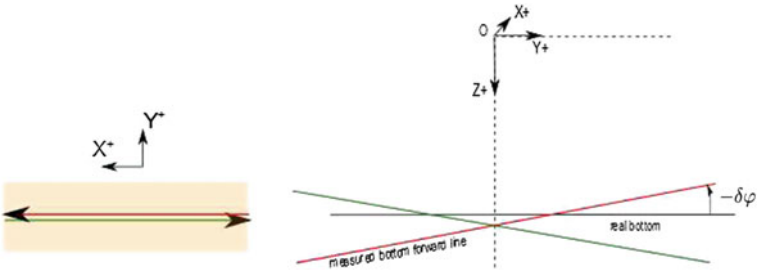

Fig. 1 Effect of roll boresight and two opposite lines on a flat seafloor. Two lines are surveyed in opposite directions; The angle between the two lines is $2\delta\varphi$. In a typical roll boresight estimation problem, the 95 % confidence interval of the estimated roll boresight that can be achieved by using a characterization method (such as estimating the angle between fitted lines or planes in the overlapping area) is about 0.05°, which is much worse than the precision of a tactical grade IMU

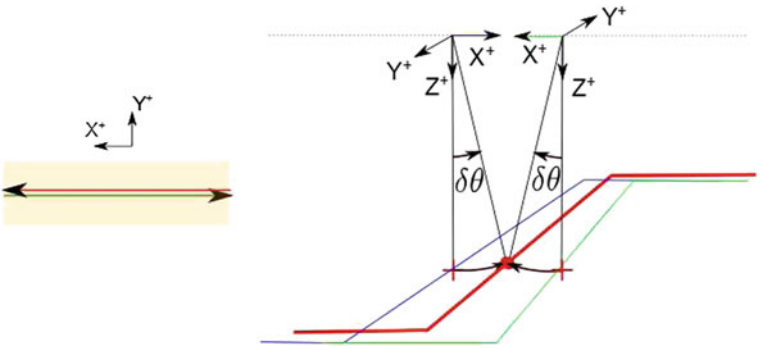

Fig. 2 Effect of pitch boresight on two opposite lines over a slope

In most data acquisition software, boresight estimation is achieved by two steps:

1. The user selects a subset of the data set from overlapping areas;
2. In reviewing all the possible boresight values over a given interval, it re-computes corrected data from source data according to the spatial referencing Eq. (1), and builds a digital terrain model (DTM) for the different overlapping data sets. Then, it compares the discrepancy between those models, and chooses the lowest one.

We observe that through this process, the choice of the analysis area dramatically impacts the boresight estimation, and is left to the user. Secondly, these methods are not properly based on optimization methods, since they massively compute all possible values of the corrected DTM for all possible values of the roll angle, the pitch angle and then the yaw angle. Consequently, they cannot deal with the problem of coupling between angles, since a true 3D computation in the boresight angles space is not achievable. Moreover, the patch-test procedure does not provide any estimate of the boresight precision, which would be highly desirable.

The effect of boresight on survey data is rather complex, with each swath being modified according to the local seafloor morphology which determines the beams grazing angles and therefore impacts the error between the actual and assumed sounding. Indeed, a boresight error acts as a rotation around the acoustic center of the MBES.

From a global point of view, the effect of boresight acts as a rotation around a time varying center (i.e., the position of the MBES). It is therefore impossible to model the effect of the boresight angle over a global surface by a simple geometric transformation like a similarity transformation for instance. In Fig. 2, the nadir beams are plotted for two opposite survey lines over a slope and flat areas. From this figure, it can be easily seen that it is impossible to deduce the actual sea floor from the assumed seafloors by a simple geometric transformation. From this remark, we deduce that boresight must be determined from a local analysis.

Another problem is the coupling between roll, pitch and yaw angles, which can be understood from the spatial referencing Eq. 1. Indeed, entries of the coordinate transformation matrix (in NED convention) $C_{bS}^{bI} = C_3(\delta\psi)C_2(\delta\theta)C_1(\delta\varphi)$ depend on the three boresight angles, which means that they contribute to each swath return distortion by coupling. We have seen that the classical patch-test method first determines the roll, then the pitch and finally, the yaw boresight. This implies that the roll boresight is determined with uncorrected pitch and yaw. In case of a non-perfectly flat sea-floor, pitch and yaw actually contribute to the MBES swath return distortion. This effect of boresight angles cross-talk has the following consequence. The determination of roll is biased by the absence of knowledge of pitch and yaw which impact data used for roll calibration over non-perfectly flat local surfaces. After roll determination, the pitch is estimated using nadir data over a slope, therefore without critical impact of roll boresight error. Yaw estimation maybe biased by the residual roll and pitch errors since it uses full swath data over a slope. It is actually the case in practice, the yaw boresight remains the most difficult to estimate, which is due to the fact the patch-test procedure uses biased data and makes inappropriate assumptions.

In summary, we have seen that

1. Each patch of non-planar surfaces is distorted by "local" rotations which depends on swath attitude angle and therefore on local grazing angles;
2. Boresight decoupling assumptions are not valid, since each boresight angle which has not yet been corrected may distort a non-planar surface.

2 Boresight Estimation Methods

As mentioned in [3], the elimination of the systematic errors from survey data can be done by two different approaches. The first consists in analyzing each component of a survey system (ranging system, inertial measurement unit, positioning system, acquisition software), and characterizing individual errors from all sensors.

Another approach is to identify systematic errors from geo-referenced data, which happens to be corrupted by coupled and non-linear combinations of sensors errors. These methods aim at retrieving systematic errors by inversion methods. Then, calibration methods fall into two main classes.

2.1 Surface Matching Methods

From several overlapping swaths, DTM surfaces are constructed, generally by using TINs (Triangulated Irregular Networks). The goal is then to find the boresight rotation matrix corresponding to the best fit of the two surfaces. Several surface matching algorithms have been proposed, see [2, 4, 7]. Examples are the Iterative Closest Point, or normal matching methods. The idea behind normal matching is to define from a DTM an orientation vector (the normal). From one surface to another (e.g., for two overlapping swaths from two points of view) alterations of the normal vectors are the basis for calibration parameter estimation. The estimation process begins based on an iterative least squares method.

2.2 Tie Point Methods

This class of methods [6, 8, 10] consists in adjusting the calibration parameters from a limited data set containing targets or control points. The drawback of these methods is that they require the *a priori* knowledge of target points, which is feasible for land survey application, but obviously not for marine survey ones. One type of such methods does not require the knowledge of geolocalized target points, but requires to be able to determine a representative position of the target (center of a sphere, for instance) from ranging data. This kind of method is employed in Terrestrial Laser Scanning applications [5], where static scans are possible, and the scanning resolution is so high that the center of a sphere can be fitted with high accuracy. This class of methods could be transposed to MBES calibration, but would impose the design of specific targets, and a radical change in MBES calibration procedures.

3 Automatic MBES-IMU Boresight Calibration

The methods we propose are based on both classes of methods presented before and the following points:

- The use of a spatial reference model taking into account boresight angles, lever-arms and other source data provided by the survey sensor suite (positioning, IMU, MBES);

- The definition of an observation equation expressing the fact that overlapping data should coincide;
- The definition of an automatic data selection process which returns appropriate overlapping subsets;
- Adjustment methods which provide numerical estimation of the boresight angles;
- Statistical analysis tools that provide external and internal reliability of the estimation process, and returns boresight angle precision.

It has been mentioned that a global surface distortion due to boresight cannot be represented by a simple geometrical transformation like a similarity transformation for example. Indeed, from Fig. 2, one can readily see that both assumed (i.e. distorted) profiles (in green and blue) cannot be transformed into the actual profile represented in red. This simple observation enables us to classify several types of boresight calibration and estimation methods:

- *Rigorous*, methods and estimation procedures which estimate the boresight coordinate transformation from elementary sounding (e.g., points) or a subset of sounding from the same swaths. Indeed, these objects are submitted to a coordinate transformation which belongs to the class of transformations we are looking for.
- *Semi-Rigorous*, methods that estimate the boresight coordinate transformation using local overlapping surfaces patches.
- *Non-Rigorous*, all other methods.

We shall say that a boresight calibration method is a decoupling method if it ignores the coupling between roll, pitch and yaw. From this classification, we can say for example that the classical patch-test is a rigorous decoupling method. Referring to normal fitting methods, widely used in LiDAR applications, we can say that they are actually semi-rigorous, but non-decoupling: Indeed, these methods estimate normal vectors to local surfaces patches constructed from overlapping data sets (i.e., they are semi-rigorous) and they adjust in 3D the boresight angles in order to fit these normal vectors (i.e., they are non-decoupling methods).

3.1 Working Limits

Our aim is to design a 3D rigorous method, which can be easily automated by analyzing relevant overlapping swath data, and which provides boresight angle precision estimation. We present here a method which seems promising from preliminary experimental results.

Let us suppose that the boresight calibration data subset is a set of overlapping swaths, over a given area. We mention here that this area needs to be defined in a sense that all boresight angles will produce significant sounding errors, in other words all boresight angles should be observable. One should avoid for instance flat areas (for which pitch and yaw are not observable) and prefer slopes. One should also

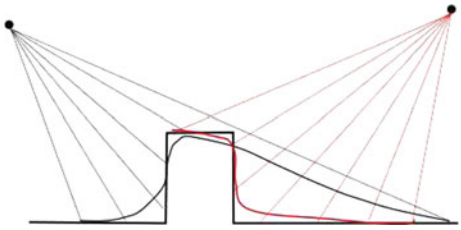

Fig. 3 Fake boresight error from overlapping data over an edge, due to different point of view and space sampling effect

avoid areas containing edges (like wrecks for instance), since the sampling effect between overlapping datasets will induce systematic boresight errors (see Fig. 3, for which we cannot distinguish a DTM error due to the sampling effect from a boresight error.

From the spatial referencing Eq. (1), assuming that latency is corrected (e.g. known from either a systemic analysis or estimated), we have the Eq. (2).

$$\mathbf{X}_n(t) = \mathbf{P}_n(t) + C_{bI}^{n}(t)[C_{bS}^{bI}\mathbf{r}_{bS}(t) + \mathbf{a}_{bI}] \tag{2}$$

For the sake of simplicity, we suppose that IMU data $C_{bI}^{n}(t)$ are not biased (i.e., the IMU is properly aligned with the local geodetic frame) and that MBES returns are not subject to launch angle and range bias. This is actually the case whenever the IMU is properly calibrated and aligned, sound speed profiles are known without uncertainty, and the surface sound velocity is correctly measured and fed into the MBES.

The parameters to be estimated are C_{bS}^{bI}, which depends on boresight angles $(\delta\varphi, \delta\theta, \delta\psi)$, and (a_x, a_y, a_z), the three entries of the lever-arm vector a_{bI}.

Let us consider a cell from a grid defined over overlapping swaths. Within every cell, we express the fact that if all points, corrected with appropriate boresight and lever-arm values lie on a given quadratic surface, then the boresight and lever-arm errors should be zero (see Fig. 4 below). From a practical point of view, if the grazing angles of the MBES swaths cover a sufficiently wide interval (i.e., if the calibration lines are run over a slope from distinct points of views), we should be able to estimate the boresight angles. In other words, the boresight angles should be observable.

3.2 Observation Equation

We detail now how this problem can be expressed as an iterative least squares problem, and how the sounding uncertainties can be propagated through this least squares problem in order to get estimates of both boresight and lever-arm precision.

Let us denote by $\mathbf{p}$, the vector of (unknown) parameters defining a quadratic surface $S(\mathbf{p}; x, y, z) = 0$, and by χ, the vector of unknown boresight angles and lever-arm

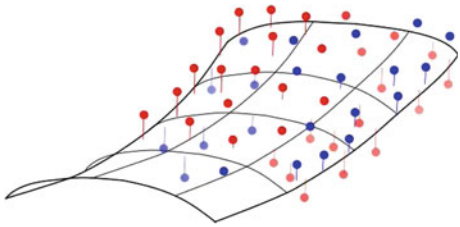

Fig. 4 Before boresight calibration, soundings from two overlapping swaths may not fit on a quadratic surface. In this example, the two point clouds do not match with any quadratic surface. In our approach, the quadratic surface and the boresight angles are adjusted in order to fit the overlapping point clouds

components. $\mathbf{p}$ can be chosen to be a 6 dimensional vector, and χ is a 6 dimensional vector. Using this notation we can write the Eq. (3).

$$\mathbf{X}_n = f(\chi; \mathbf{P}_n(t), C_{bI}^n(t), \mathbf{r}_{bS}(t)) \tag{3}$$

where $\mathbf{P}_n(t), C_{bI}^n(t), \mathbf{r}_{bS}(t)$ are here considered as external data depending on each sounding measured at time t. The criterion we use to determine both $\mathbf{p}$ and χ is expressed in the Eq. (4).

$$S(\mathbf{p}; f(\chi; \mathbf{P}_n(t), C_{bI}^n(t), \mathbf{r}_{bS}(t))) = 0 \tag{4}$$

Equation (4) express the fact that the point $\mathbf{X}_n(t)$ lies on a given quadratic surface. Let us now consider the collection of conditions, for all overlapping points of a given grid, defined on the horizontal plane. After linearization, this system, can be written as a least squares problem that can be solved by an iterative procedure, and enables both external and internal reliability analysis.

4 Numericals Results

We present some results, obtained from the application of the method presented above from calibration lines performed with an hydrographic system composed of an R2SONIC 2022, an IXBLUE OCTANS4, and a MAGELLAN proflex500 GNSS receiver. The data acquisition software used was QINSy. These tests have been conducted by the ENSTA Bretagne hydrographic team over a slope located in the Brest harbor.

Let us first mention that the geometry of line and overlaps used by our method is different from the classical patch-test method. Indeed, we need to guarantee boresight angle observability, which can be achieved only with a set of swaths obtained from significantly different points of view of the same area. Therefore, a set of cross-

Table 1 Calibration numerical results in the Brest harbor

Boresight angles [°]	Roll ($\delta\varphi$)	STD	Pitch ($\delta\theta$)	STD	Yaw ($\delta\psi$)	STD
Patch-test	0.62	?	1.64	?	1.88	?
ABE	0.679	0.006	1.657	0.002	1.995	0.03

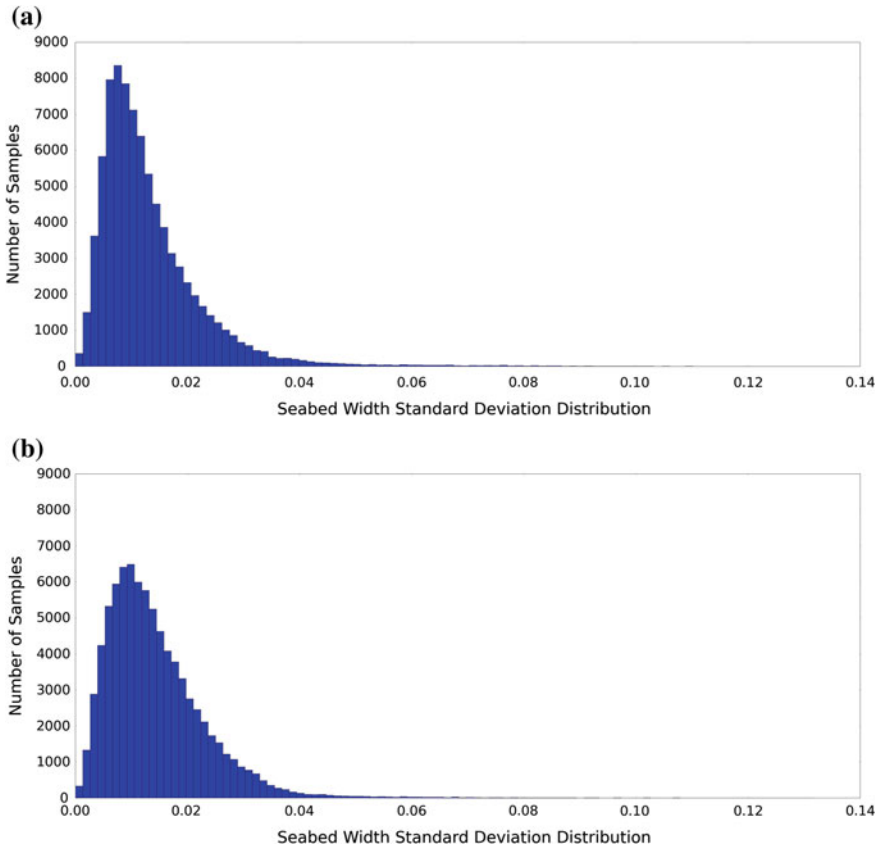

Fig. 5 From the two histograms, one can see that the automatic boresight method (**a**) provides a better global fit of overlapping data. Indeed the plot shows number or samples versus the adjustment error. **a** seabed width standard deviation histogram with estimated boresight angles correction. **b** seabed width standard deviation histogram with Patch-test boresight angles correction

ing lines over a slope has been surveyed. In order to compare our approach with the patch-test, we also performed patch test lines (over flat surfaces for roll, and the same slope for pitch and heading), and estimated calibration parameters with classical software tools. Table 1 presents the values of the boresight angles found by Automatic Boresight Estimation (ABE) and the classical patch-test.

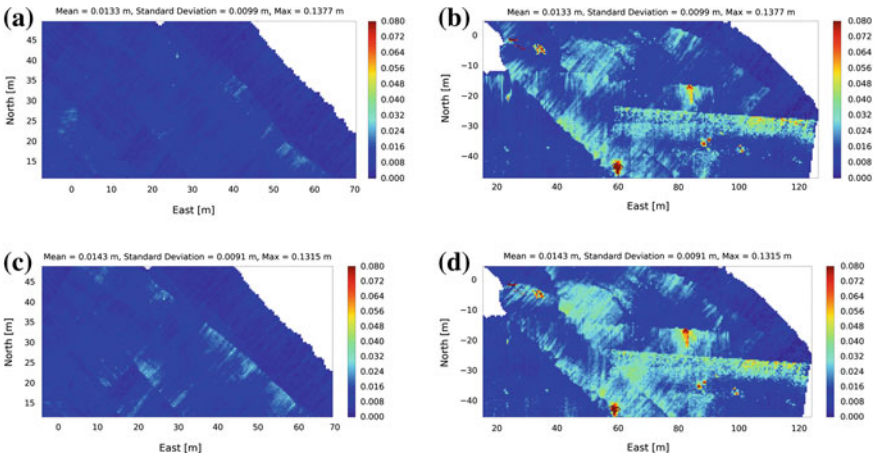

Fig. 6 Global data set precision estimation, for the boresight estimated by our automatic method (*top* with **a** and **b**) and a classical patch test (*bottom* with **c** and **d**). By observing the two selected areas, one can see that the automatic method is performing better. **a** seabed width standard deviation with the estimated boresight angles correction on a flat area. **b** seabed width standard deviation with the estimated boresight angles correction on a mix flat/slope area. **c** seabed width standard deviation with the Patch-test boresight angles correction on a flat area. **d** seabed width standard deviation with the Patch-test boresight angles correction on a mix flat/slope area

As a measure of the precision of the bathymetric surface built with a given boresight value, we use the following process: For each cell of a grid, we fit a plane by total least square (TLS) and use the orthogonal error of the point cloud which is given by the lowest singular value computed by the TLS. The advantage of this method with respect to the classical standard deviation map is to cancel out the effect of local slope.

Figure 5 shows the histogram of the orthogonal error (i.e., seabed width standard deviation) for both our approach and a classical patch test. Figure 6 presents the chart results obtained using the calibration results of the Table 1.

It is to be mentioned that the proposed approach is in theory able to estimate both boresight angles and lever-arms values through the same optimization process. However, from our preliminary results, it seems that the joint estimation of all these parameters is difficult from a practical point of view. Indeed, in order to obtain the observability of the boresight angle, we need significantly different points of view of a given smooth slope. In order to get lever-arm observability, we need relatively high attitude angles, again over a slope. It appears that our dataset contains only relatively high attitude angles over a moderate slope, and different overlapping lines over a sharp slope, but only with small attitude angle.

As a consequence, we see that we cannot systematically estimate both the boresight angle and the lever-arms from the same overlapping raw data, as observability of these parameters depends on source data. Therefore, the methodology we propose for the practical use of this approach is:

1. Estimate lever-arms from a data set selected using a lever-arm observability criterion;
2. Estimate the boresight angles from another area, selected using a boresight observability criterion.

5 Conclusion

The new calibration procedure introduced in this paper provides promising preliminary results. The use of an observation equation and least-squares optimization method allow working on the boresight problem source. Furthermore, the linearization of an observation equation gives us the possibility to use the statistical analysis toolbox of least-squares. All these aspects give the essential information (value, precision, internal and external reliability...) which should be in a calibration report. Moreover, this procedure, being automatic, allows the hydrographer to save time at sea.

The results presented need to be confirmed by other tests with different systems and other survey areas. The boresight angles estimation is reliable but the lever-arms estimation needs to be investigated in order to be included in a new global procedure.

References

1. Calder B. R., Brennan R. T, Malzone C., Marcus J., & Canter P. (2007). Application of High-Precision Timing to Distributed Survey Systems, *Proceedings of the US-Hydro Conference, Norfolk, VA*.
2. Filin, S. (2003). Recovery of systematic biases in laser altimetry data using natural surfaces. *Photogrammetric Engineering and Remote Sensing*, *69*, 1235–1242.
3. Filin S., & Vosselman G. (2004). Adjustment of airborne laser altimetry strips. In: *ISPRS Congress Istanbul, Proceedings of Commission III*.
4. Glennie, C. (2007). Rigorous 3d error analysis of kinematic scanning lidar systems. *Journal of Applied Geodesy*, *1*, 147–157.
5. Grejner-Brzezinska, D. A., Toth, C. K., Sun, H., Wang, X., & Rizos, C. (2011). A robust solution to high-accuracy geolocation: Quadruple integration of gps, imu, pseudolite, and terrestrial laser scanner. *IEEE Transactions on instrumentation and measurement*, *11*, 3694–3708.
6. Kumari, P., Carter, W. E., & Shrestha, R. L. (2011). Adjustment of systematic errors in als data through surface matching. *Advances in Space Research*, *47*, 1851–1864.
7. Morin K., & El-Sheimy, N. (2002). Post-mission adjustment methods of airborne laser scanning data. In: *FIG XXII International Congress, Washington DC*, 19–26 Apr 2002.
8. Schenk, T. (2001). Modeling and analyzing systematic errors of airborne laser scanners. Technical report, Department of Civil and Environmental Engineering and Geodetic Science, The Ohio State University, Columbus, OH.
9. Seube, N., Picard, A., & Rondeau, M. (2012). A simple method to recover the latency time of tactical grade IMU systems. *ISPRS Journal of Photogrammetry and Remote Sensing*, *74*(2012), 85–89.
10. Skaloud, J., & Litchi, D. (2006). Rigorous approach to boresight self-calibration in airborne laser scanning. *ISPRS Journal of Photogrammetry and remote Sensing*, *61*, 47–59.

http://www.springer.com/978-3-319-32105-9

Quantitative Monitoring of the Underwater Environment
Results of the International Marine Science and Technology Event MOQESM´14 in Brest, France
Zerr, B.; Jaulin, L.; Creuze, V.; Debese, N.; Quidu, I.; Clement, B.; Billon-Coat, A. (Eds.)
2016, XVII, 131 p. 87 illus., 69 illus. in color., Hardcover
ISBN: 978-3-319-32105-9